



Research Article

Experimental investigation of forced convective heat transfer and fluid flow in a mini heat pipe with rectangular micro grooves

Bassim Mohammed MAJEL¹, Zain Alabdeen Hussein OBAID^{2,*}

¹Department of Refrigeration and Air-Conditioning Engineering, Al-Rafidain University College, Baghdad, Iraq

²Renewable Energy Research Centre, University of Anbar, Ramadi, Iraq

ARTICLE INFO

Article history

Received: 25 May 2022

Accepted: 06 September 2022

Keywords:

Heat Pipe; Two-Phase Flow; Integrated Circuits; Heat Transfer Coefficient

ABSTRACT

In the present study, the convective heat transfer coefficient of water in a laminar flow regime under constant inlet temperature conditions inside a flat mini heat pipe was investigated experimentally. Heat flux ranged from 20-50W and various horizontal heat sink temperatures (operating temperature) ranged from 15-35°C with liquid flow rate ($3.563E-8$ m³/sec) used during the experiments. The rectangular microchannels performance is evaluated in terms of the temperature profile, heat transfer coefficient, Nusselt number and thermal resistance. The results emphasized that the mini heat pipe temperature gradients are less than the temperature of the copper plate and the heat resistance gradually decreases to its lowest value when the heat flux value reaches its highest value if it does not exceed the capillary limits. The data also demonstrated that the coefficient of heat transfer in the condensation zone is lower than in the evaporation zone at different heat sink temperatures. The augmentation rate for the flat mini heat pipe thermal conductivity reached about 240% at a heat load 30W for the positions of thermosyphon and horizontal, while the rate of increase in the case of the anti-gravity situation at a heat load 30W reaches 210%, then the improvement percentage begins to decrease to 200%. A generalized regression equation is developed for the estimation of the Nusselt number valid for water in a flat mini heat pipe.

Cite this article as: Majel BM, Obaid ZAH. Experimental investigation of forced convective heat transfer and fluid flow in a mini heat pipe with rectangular micro grooves. J Ther Eng 2024;10(1):207–218.

INTRODUCTION

To achieve a thermally efficient and financially viable design, heat exchangers with natural and forced convection may transfer heat more quickly [1-5]. Thermal administration of electronic parts should take care of issues associated with the impediments on the most extreme temperature of chip and the prerequisites of the degree of temperature

consistency. For cooling electronic parts, one can utilize fluid coolers and air just as coolers built on the standard of the stage change heat move in shut space, for example, submersion, thermosyphon and coolers of heat pipe. Every one of these techniques has its benefits and downsides because in the decision of fitting cooling one should think about the cooler thermal parameters, price, durability and application [1].

*Corresponding author.

*E-mail address: zaobaid@uoanbar.edu.iq

This paper was recommended for publication in revised form by Regional Editor Tolga Taner



Heat pipes consider a suitable solution for electronic hardware cooling, so it is used to cool computer electronic parts. It is a closed system and its ability to transfer heat depends on the working fluid besides the structure design. A few narrow designs are created to meet explicit warm necessities. They are established either by an incorporated construction of microgrooves or microchannels machined in the inner surface of the warmth spreader or by permeable designs made of sintered powders or wire screens. As per certain conditions, made fine designs can be incorporated into heat pipes. Flat miniature heat pipes are little effective gadgets to meet the necessity of cooling electronic parts. They are created in various methods depending on the used material, the precision fin design and the technology used in the manufacturing process. The current review manages the improvement of a flat miniature heat pipe idea and how it is used to cool high thermal scattering electronic parts. Experimental tests are done to calculate the performance of heat pipes based on different parameters. By looking at the exploratory results with the calculated data, the dependability of the mathematical model can be checked [6].

For flat miniature heat pipes comprised of an incorporated fine design including capillary channels of various shapes, the hypothetical methodology comprises concentrating on the flow stream and the transfer of heat in insulated channel surfaces. The influence of the main variables on which the flat miniature heat pipe depends can be calculated by experimental investigation. Thus, the impact of the working fluid, the interaction between vapour and the base fluid, the capillary channel geometry and hydraulic diameter can be calculated by analysing the thermal and hydrodynamic boundary layer of the selected test section [7].

Microchannel cooling technology was introduced to the world by *Tuckerman and Pease* [8]. They flowed water in a microchannel created in silicon chips and the maximum value of a heat flux they were able to reach was $790\text{W}/\text{cm}^2$ without any change in phase with a pressure drop of 1.94 bar. *Amer et al.* [9] discovered that the number of Nusselt depends on the Reynolds number in laminar microchannels flow [10]. This was observed clearly from their simulation with the use of microchannels inside diameters ranging from 3 to $81\mu\text{m}$. *Khrustalev and Faghri* [11] conducted an experimental investigation to determine the heat transfer and fluid flow characteristics in a rectangular microchannel under two-phase flow conditions. The pressure drop and the coefficient of friction factor had been studied during the experiment and analysed the interaction between the vapour and the working fluid. The data illustrated that the influence of the interaction of the vapour-liquid frictional on the stream of flow decreases with the interface curvature of the liquid-vapour and the shear stress decreases as we go to the centre and its irregular at the interface between the liquid and vapour. *Qu and Mudawar* [12] conducted an experimental study to investigate the coefficient of saturated flow under two-phase flow conditions. The water is used as a coolant in microchannel heat sinks of 21 parallel

microgrooves having $(231 \times 713\mu\text{m})$ dimensions. A specified model of annular flow was developed to predict the coefficient of boiling heat transfer. Micro-channel two-phase features such as laminar vapour flow and droplet entrainment are incorporated into the correlation. The experimental data showed that the coefficient of heat transfer in boiling condition is a strong function of the mass boiling flow rate and it does not depend too much on the heat flux. This proves the hypothesis that the process of heat transfer mechanism is not highly dependent on nucleate boiling, but rather depends on convective boiling.

Steinke and Kandlikar [13] investigated theoretically and experimentally the fundamental characteristics of boiling heat transfer in six horizontal and parallel microchannels with a hydraulic diameter of $207\mu\text{m}$. The water was used as a coolant with an inlet temperature of 22°C and mass flux ranging from 157 to $1782\text{ kg}/\text{m}^2\cdot\text{s}$ and different ranges of uniform thermal power from 5 to $930\text{ kW}/\text{m}^2$. The visualization of flow was used to study the reversal flow. The data indicated that the local coefficient of heat transfer decreases with the increase in quality and nucleate boiling has a big role in the heat transfer process. *Launay et al.* [14] evolved a mathematical model to predict the ability of heat transfer and distribution of temperature along the flow line of a flat miniature convective heat pipe using water as a working fluid. The energy of heat transfer and fluid flow have been combined to study the evaporating and condensing conditions in thin films. The distributions of temperature, pressure drop and velocity were calculated during the two phases liquid and vapour. The index of thermal performance for the system has been simulated based on constant boundary conditions of a flat miniature convective heat pipe condenser and evaporator. The influence of the dry-out on the flat miniature convective heat pipe performance can also be predicted based on the fluid fill charge and the boundary conditions. *Saitoh et al.* [15] performed experiments to study the boiling convective heat transfer and fluid flow in horizontal tubes of diameters 0.51 , 1.12 , and 3.1 mm , respectively. The refrigerant R-134a was used as a coolant during the study. The mass flux ranges from 150 to $450\text{ kg}/\text{m}^2\cdot\text{s}$ with a constant input power ranged from 5 to $39\text{ kW}/\text{m}^2$. The quality of vapour varied from 0 to 0.2 and the temperature of evaporating changed from 278.15 to 288.15 K . The local coefficient of convective heat transfer and drop of pressure were calculated during the experiments. The results indicated that the local coefficient of convective heat transfer decreases with the diameter of the tube decreasing at a lower quality of vapour and the influence of mass flux on the local coefficient of convective heat transfer decreases with the diameter of the tube decreasing. The uniform heat flux has a big role in three selected diameters. The flow inside the tube became homogeneous when the diameter of the tube decreased and the heat transfer by evaporation to the boiling heat transfer decreased with the inner tube diameter decreasing.

Do et al. [16] proposed a typical model to predict the thermal performance of flat miniature heat pipe in

rectangular microchannel. The influence of shear stress on the vapour-liquid interfacial, the mass flux and the angle of contact are calculated in the study. Young-Laplace and 1-D conduction equations are solved to calculate the surface temperature along the axial flow direction, condensation and evaporation rates. The results demonstrated that the assumptions that were used in the model led to major errors in the thermal performance calculation and the simulated data are in good agreement with experimental results in the literature. The maximum rate of heat transfer is improved by 20% for the optimum conditions, as compared to the data from the experiments. *Bertsch et al.* [17] studied the convective heat transfer in a boiling state using R-134a and R-245fa as coolants inside rectangular microchannels made from copper with an aspect ratio of 2.5. Different hydraulic channel diameters are considered during the investigation. The local coefficient of heat transfer was obtained depending on various ranges of vapour quality up to 0.9 with inlet temperature at saturation conditions ranging from 8 to 30°C. The supplied constant heat flux ranges from 0 to 22 W/cm² with various ranges of mass flux from 20 to 350 kg/m².s. The data showed that the heat transfer by nucleate boiling dominated the process and the quality of vapour and heat flux has a great effect on the coefficient of heat transfer.

Do and Jang [18] calculated the thermal performance of a flat miniature convective heat pipe using Alumina nanofluid as a coolant in a rectangular array minichannels. Young-Laplace and 1-D conduction equations are solved to calculate the wall temperature along the axial flow direction, condensation and evaporation rates for the phase change process. The results demonstrated that the thermal performance of the heat pipe with the presence of nanofluid Al₂O₃ is higher than when using water and as the nanoparticle concentration increases the thermal performance increases. The data showed that there is potential to further improve heat transfer up to 100% by using nanofluids at a concentration lower than 10%. The results also demonstrated that the thermal resistance decreases with the increase of nanoparticle size. More information about using nanofluid in heat transfer enhancement can be found here [19 and 20]. *Sylwia et al.* [21] studied the heat transfer boiling characteristics in a parallel microchannels heat sink using three types of coolant as a working fluid R245fa, R236fa, and R1234ze. The cross-sectional area of microchannels is 100×100 μm², the length of each channel is 10 mm and the evaporator consists of 67 longitudinal channels. Great inverse flow, unstable flow and irregular flow were observed in the microchannel despite the absence of obstacles in the flow area, therefore the rectangular obstacles were set at the inlet of the channel to prevent these problems from happening. Tests showed that the boiling onset at lower input power because of the flashing influence and the thermal input power for a high range of 48.6 W/cm² could be dissipated while keeping the temperature of the micro-evaporator below 85°C. *Leão et al.* [22] investigated experimentally the convective heat transfer in two-phase

flow inside 50 parallel rectangular channels of dimensions ranging from 100 x 500 μm², and the channel length of 15mm under uniform heat fluxes up to 310 kW/m². A coolant of R407C was used as a working fluid with mass flux ranging from 400 to 1500 kg/m².s under sub-cooling conditions for the inlet flow of 5, 10 and 15°C and the inlet saturation temperature of 25°C. The data demonstrated that the thermal performance of the heat sink enhances with the decreasing of mass flux while the average coefficient of heat transfer increases with the mass flux increasing. The estimated average coefficient of heat transfer reaches up to 30 kW/m².°C during the boiling state.

This paper investigates the thermal performance and design of a flat mini heat pipe as an effective supporting shelf for integrated circuit boards of computer components to dissipate and transport heat away to the aluminium enclosure. In this paper, one identical configuration was designed and tested, Therefore, it was the objective of this investigation to extensively manufacture, experimentally investigate and theoretically model a variety of flat miniature heat pipes. In particular the experimental investigation will mainly seek out the maximum heat flow rates and heat fluxes that can be applied uniformly to the evaporator wall for a range of operating temperatures, orientations and heating configurations. The predictive model is developed to predict the capillary limitation of all investigated flat miniature heat pipes while a closed form solution of the predictive model is also included for the limiting case of axial rectangular grooved flat miniature heat pipes.

EXPERIMENTAL INVESTIGATION

Heat Pipe Manufacturing

The test rig has been fabricated and designed based on some electronic criteria associated with the heat sink which needs to dissipate the largest amount of heat generated due to operation. More restrictions such as heat sink weight, size and total system temperature were taken into account when designing the test model. The test section is made from copper with dimensions of width, length and thickness of 60mm, 120mm and 4mm, respectively. The body of the system was fabricated in two halves, in the first half of thickness (3mm), rectangular capillary grooves (0.5 x 0.5mm²) were made by a CNC machine, while the second half of thickness (1mm) was welded to the first part using beam of laser. The coolant is charged to the test rig by a heat pipe charging tube of diameter (2.5mm) which is welded to the end of the heat pipe by a normal welding method. The boiling filling process needs to boiler, vacuum valve, and vacuum system, and to charge the working fluid to the system, some important steps must be taken: Empty the system from the air by boiling process, then ensure that system is fully vacuumed and at the end, the flat heat pipe is charged with optimum liquid amount about (1.5ml). The tested flat heat pipe with dimensions are indicated in Figure (1).

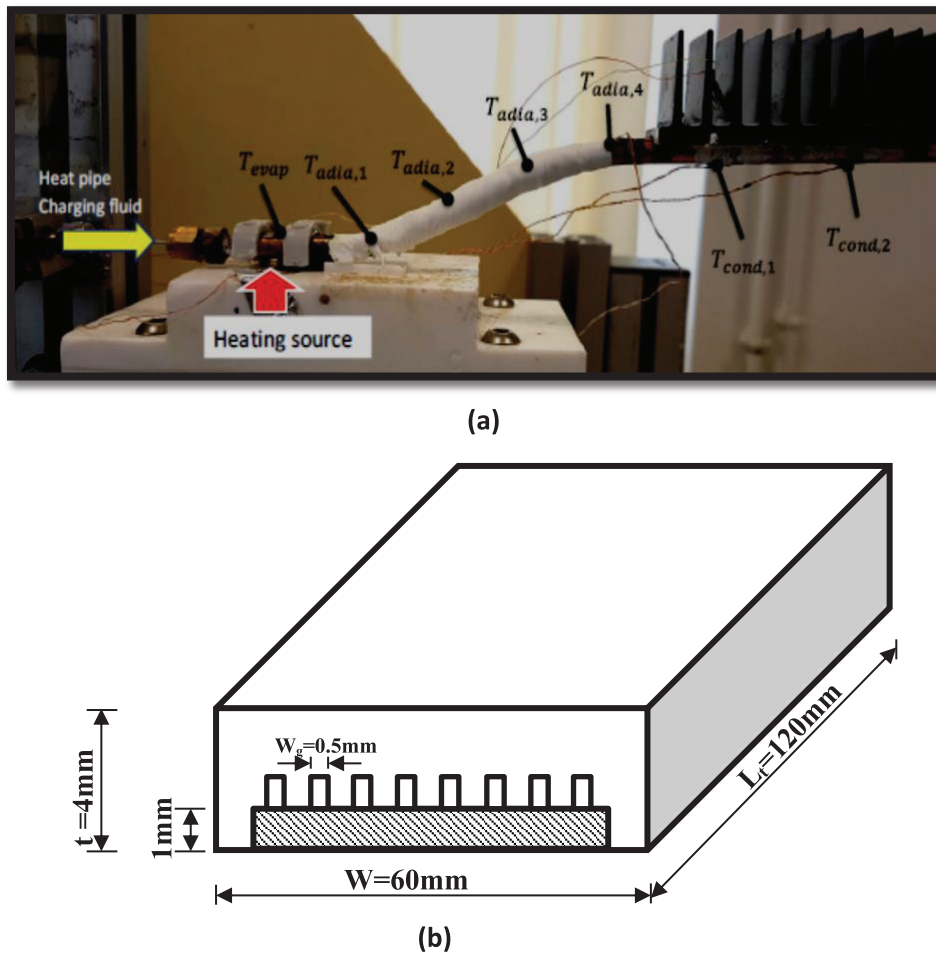


Figure (1). (a) Heat pipe test rig, (b) Heat sink and microgrooves dimensions.

Table 1. Geometric dimensions of a flat mini heat pipe

FMHP Width (W)	Groove Width (W_g)	Groove Spacing (S_g)	Groove Height (D_g)	FMHP Thickness (t)	Groove Number (N_g)	FMHP Length (L_t)
60mm	0.5mm	1mm	0.5mm	4mm	53	120mm

Experimental Apparatus and Procedures

To conduct the experimental investigations, the test apparatus is established for the experimental studies as shown in Figure (2). Thermal input power was supplied by the heater located at the end of the flat mini heat pipe and the constant heat flux was controlled by a variac to the test section a digital Avometer was used to measure the voltage and current during the tests. A cryostat is a device used to maintain low temperatures of samples or devices mounted within the cryostat. Low temperatures may be maintained within a cryostat by using various refrigeration methods, most commonly using cryogenic fluid bath such as liquid helium. The adiabatic side and the evaporator were

insulated with thermal insulation and the thermal losses from the isolated part were calculated by finding the difference in temperature between the insulated surface and the outer perimeter. Water was used to dissipate the heat from the system and a material with high thermal conductivity is placed between the aluminium blocks and the copper side. The heat flux has been increased from a small value to a value at which the temperature of the evaporator begins to increase suddenly and the temperature distribution of the pipe was recorded by thermocouples. Eight thermocouples type-J are distributed from the evaporator end cap section to measure the surface temperature of the flat mini heat pipe and to measure temperatures of the condenser and

evaporator holes were made on the wall of the flat mini heat pipe and thermocouples were distributed on it. The flow rate was adjusted to start the experimental procedures and the evaporator section was heated gradually using a variable transformer to generate constant heat flux. The temperature of the aluminium heat sink was maintained by adjusting the flow rate of the coolant (water). The experiment was running for (20-25 minutes) until it reach steady-state condition and after that, the temperature read out through the type-J thermocouples is recorded and thermal input power is increased to reach the required heat flux. For each step of thermal input power, all results were recorded after reading the sensors and reaching a steady-state using

data acquisition type IMP35951 and Lab VIEW software. All thermocouples were calibrated and the calibration accuracy was ranged from ($\pm 0.3-0.5^{\circ}\text{C}$). The thermal input power produced from the heater from the mathematical relation ($Q = V \times I$) and thermal resistance (R_{th}) of flat mini heat pipe is calculated from the ratio of the temperature difference across the flat mini heat pipe to the thermal input power (Q). The thermocouples distribution is shown in Figure (3).

Data Reduction

The following mathematical expression is utilized to obtain the coefficient of heat transfer in the zones of the condenser and evaporator [23]:

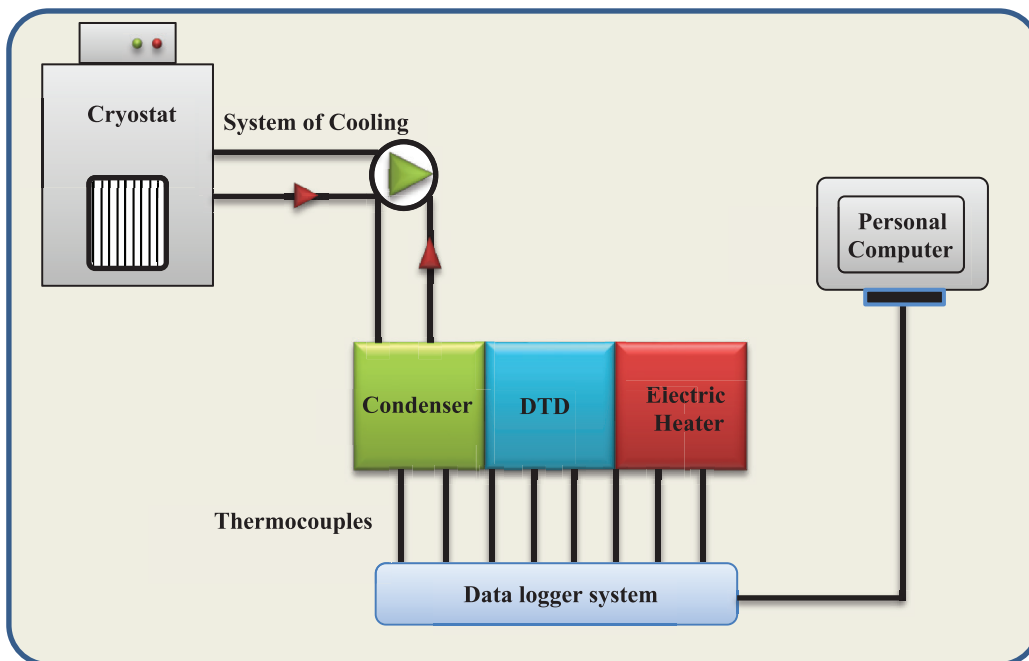


Figure 2. The main components Sketch of the test rig.

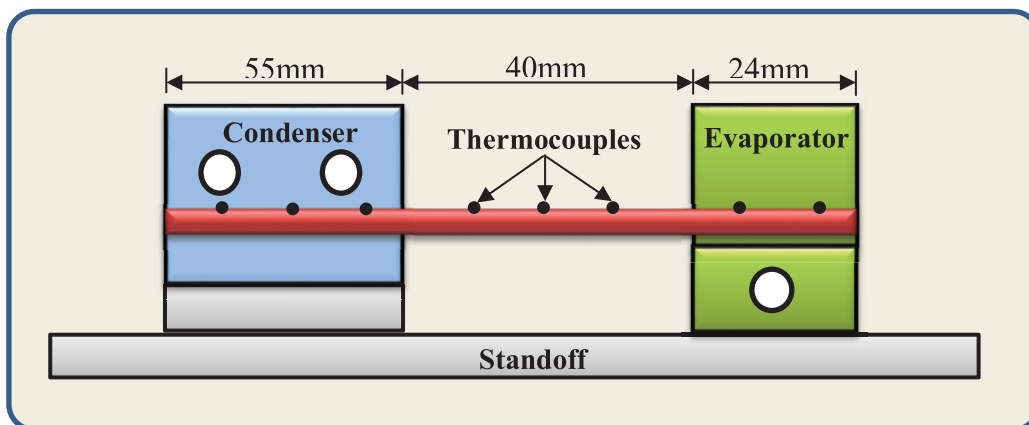


Figure 3. Location of thermocouples distribution.

$$h_{Evaporator} = \frac{1}{((T_{ev} - T_{sat})/q_{ev}) - (t_w/k_w)} \quad (1)$$

$$h_{Condenser} = \frac{1}{((T_{sat} - T_c)/q_c) - (t_w/k_w)} \quad (2)$$

Experimental data is processed and converted to dimensionless numbers to get the laws of boiling convective heat transfer based on the theorem of Vaschy-Backingham, and the constant of Laplace is [23]:

$$La = \sqrt{\frac{\sigma}{(\rho_l - \rho_v)g}} \quad (3)$$

Then dimensionless Reynolds number is [23]:

$$Re = \frac{\rho_l V_e La}{\mu_l} = \frac{q}{\mu_l \Delta h_v} \quad (4)$$

Dimensionless Prandtl number is [23]:

$$Pr = \frac{\mu_l C_{p_l}}{k_l} \quad (5)$$

And Nusselt number [23]:

$$Nu = \frac{h La}{k_l} \quad (6)$$

Where h: Coefficient of heat transfer in condenser and evaporator zones.

The adjusted Jakob number [23]:

$$Ja = \frac{C_{p_l} T_{sat} \rho_l}{\Delta h_v \rho_v} \quad (7)$$

Hence, the average Nusselt number can be found from the following empirical correlation[23]:

$$Nu = C Re^{u_1} Pr^{u_2} Ja^{u_3} \quad (8)$$

Where: C, u_1 , u_2 , and u_3 are constant, and their value is calculated from the experimental results by analysis of linear regression.

RESULT AND DISCUSSION

Variation of Nusselt Number

The comparison between the experimental average Nusselt number and the analytical average Nusselt number obtained from equation No. (8) is depicted in Figure (4). From this figure, it is clear that in the case of the evaporation boiling heat transfer zone (b), there is a good compatibility between the Nusselt values that were obtained experimentally and those obtained from equation No. (8), and the largest deviation between these values is $\pm 13\%$. For the condensation boiling heat transfer zone (a), the maximum deviation recorded is $\pm 8\%$.

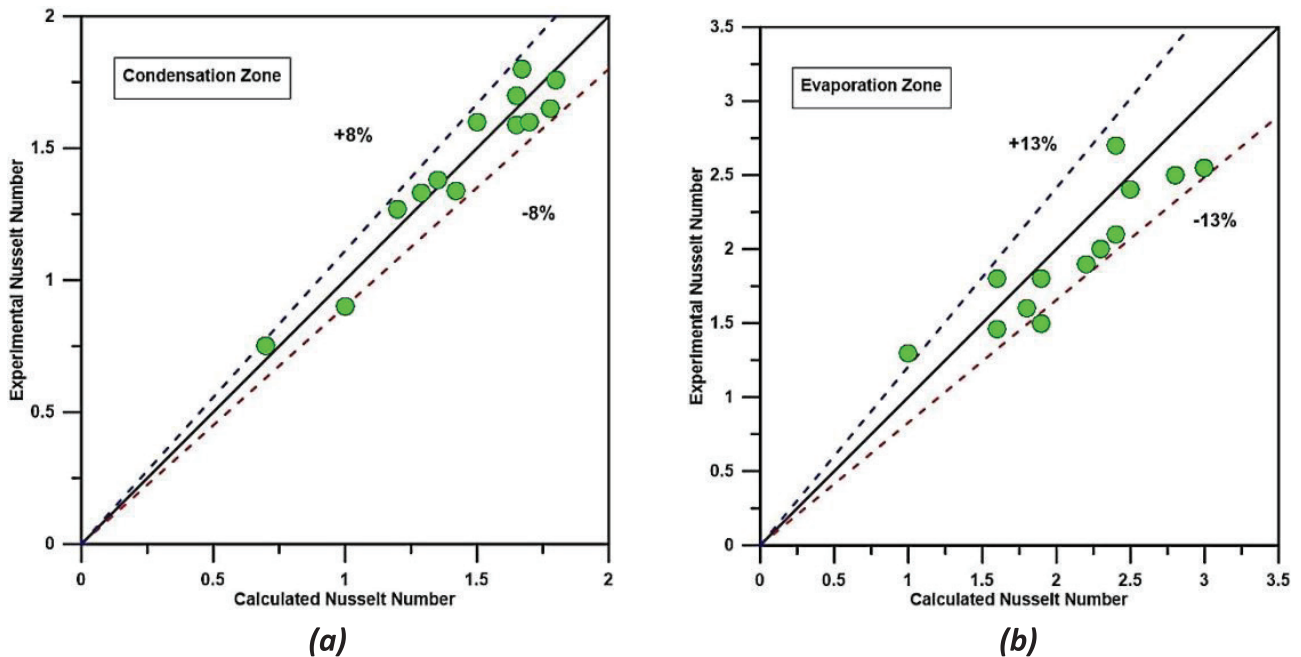
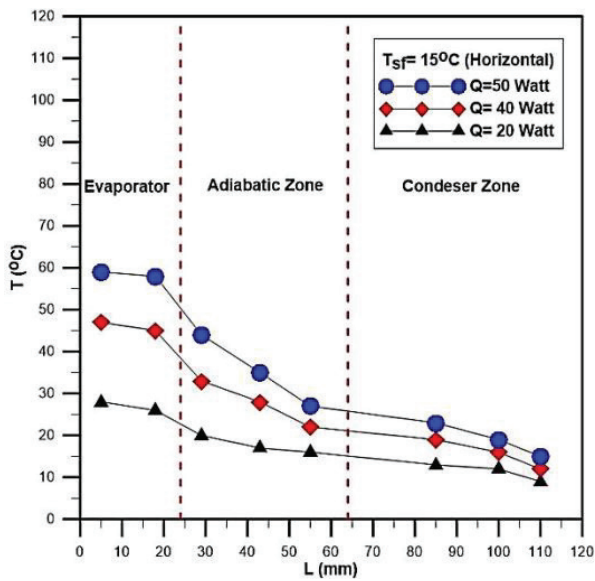


Figure 4. Experimental average Nusselt number versus analytical average Nusselt number (a) condensation zone, (b) evaporation zone.

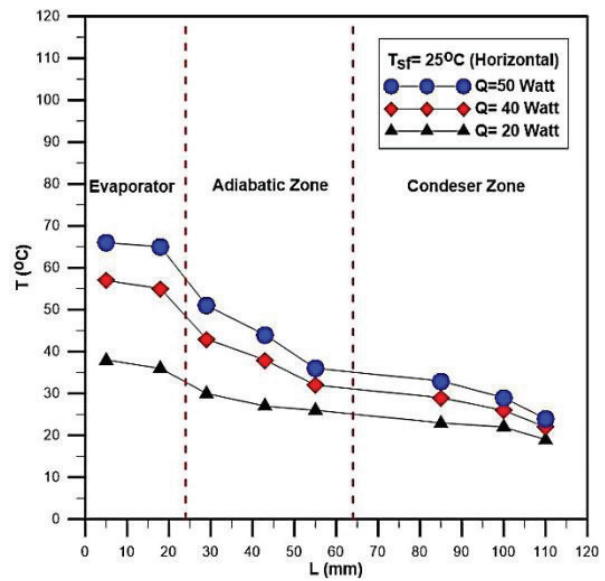
Dual Influences of the Dissipation Unit Temperature and Heat flux

Figures (5a – 5c) demonstrate the axial distance temperature distribution for flat mini heat pipe at various values of heat flux ranging from 20-50W and different temperature degrees for horizontal heat sink ranging from 15- 35°C. From these figures, it can be seen clearly that the highest value of the evaporator temperature for a flat mini heat pipe is lower than the temperature of the copper piece which is illustrated in the Figure (5d).

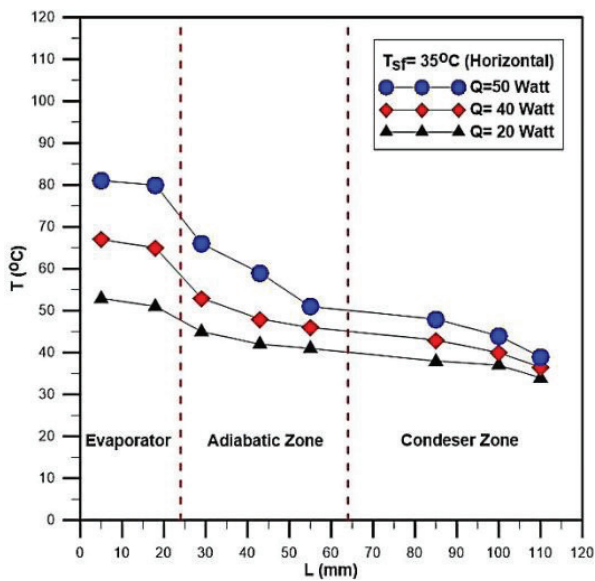
The wall temperature difference between the evaporator and condenser for heat sink temperature $T_{sf} = 35^\circ\text{C}$ is shown in Figure (6) as a function of heat flux in horizontal position and the temperature difference for a plate of copper is also illustrated in order to compare with the temperature difference of the flat mini heat pipe. The diagram shows that the temperature gradients of the mini heat pipe are less than the temperature of the plate of copper. As illustrated in Figure (6), the process lowers the temperature slope gradient of the flat mini heat pipe and this gives



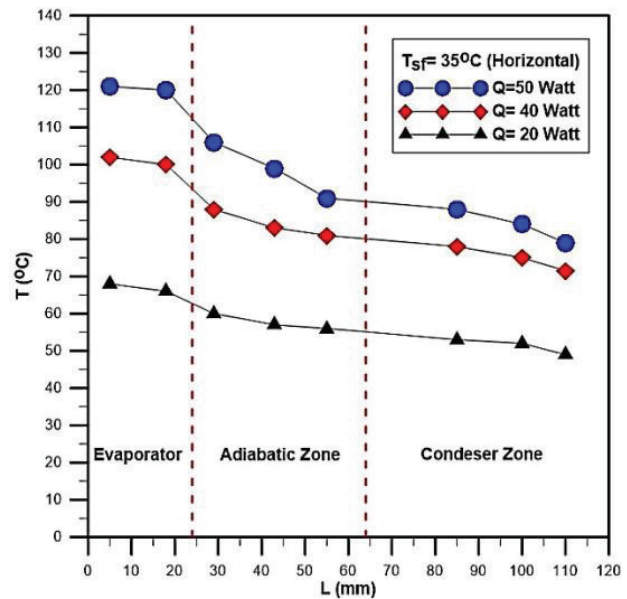
(a)



(b)



(c)



(d)

Figure 5. Temperature distribution of flat mini heat pipe at different heat sink temperatures: a) $T_{sf} = 15^\circ\text{C}$. b) $T_{sf} = 25^\circ\text{C}$. c) $T_{sf} = 35^\circ\text{C}$. d) Temperature distribution for copper plate at $T_{sf} = 35^\circ\text{C}$.

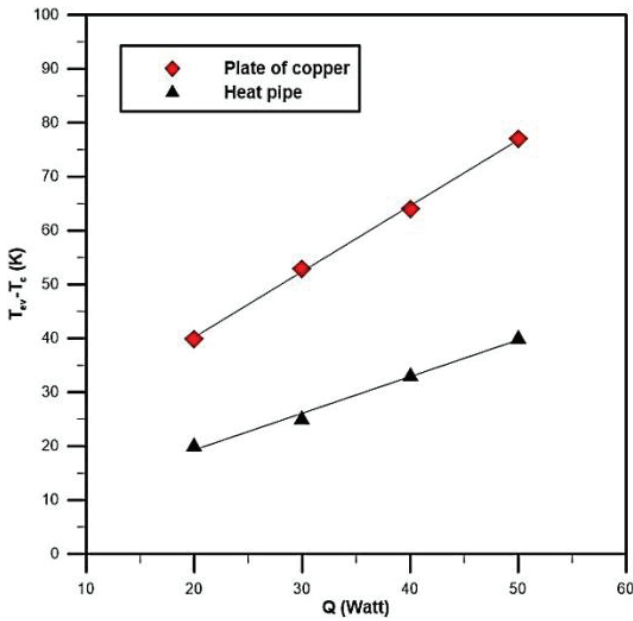


Figure 6. Temperature difference variations versus thermal input power.

us an impression of the ability of the heat pipe to lowering temperatures in hot areas. The temperature difference variations increases as the thermal input power increase, for example, the difference increases from 19°C at 20 W heat flux to approximately 35°C at a heat flux 50W.

Figure (7) shows the flat mini heat pipe’s effective thermal resistance versus the thermal input power and the thermal resistance has great value at low heat flux as stout liquid film located in the evaporator zone. From the Figure, it is clear that thermal resistance gradually decreases to its lowest value when the heat flux value reaches its highest value and when the thermal input power increases more than the limit of the capillary the thermal resistance begins to increase as the evaporator is almost devoid of liquid. This situation occurs due to the inability of the pumping power to defeat the losses in pressure. The decrease in thermal resistance of flat mini heat pipe is mainly due to the decrease in thermal resistance of the evaporator at a high heat flux value. In fact, the increased heat input power enhances the evaporation process in the channels. The process of intense boiling can occur if the value of the heat flux exceeds the capillary limits and as a result, the thermal resistance of the evaporator will increase. This leads to an increase in the thermal resistance of the flat mini heat pipe.

The effective thermal conductivity (k_{eff}) of the flat mini heat pipe is calculated based on Fourier’s law. The thermal input power rate is calculated by dividing the heat load over the area of the cross-sectional mini heat pipe. The extracted value is then divided over the temperature difference and then the results obtained is multiplied by the distance between the measured heat sink– source temperature points. Figure (8) shows that this increase in the effective

thermal conductivity for flat mini heat pipes is due to the low-temperature gradient that occurs when the thermal flux increases and this makes the heated pipes work more efficiently.

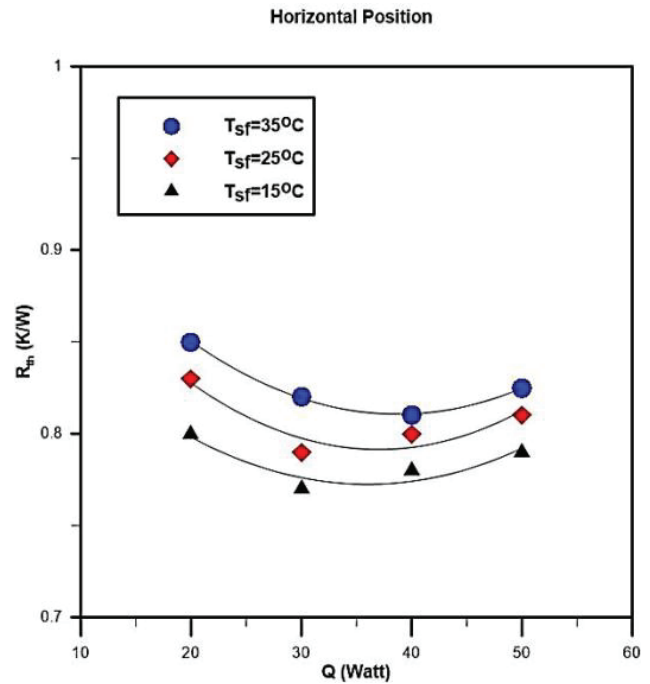


Figure 7. Flat mini heat pipe thermal resistance versus heat load.

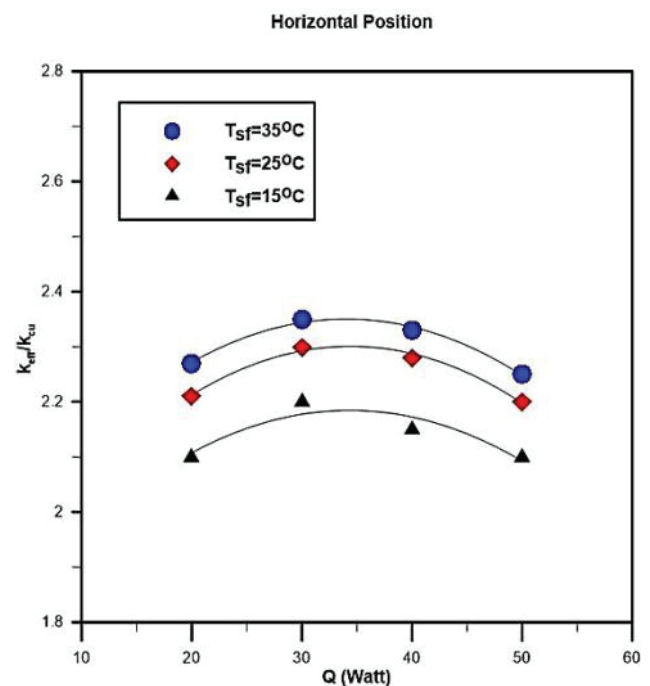


Figure 8. Augmentation of effective thermal conductivity versus heat load at various heat sink.

The heat transfer coefficient variations for condenser and evaporator zone versus heat load are shown in Figure (9). The Figure depicts that the coefficient of heat transfer in the condensation zone is lower than in the evaporation zone at different heat sink temperatures. In fact, the evaporation deterioration process results from the evaporator being free of liquid at high heat flux values higher than the limit of capillary and as a result, dehydration occurs, and therefore the pumping power is insufficient to prevent the pressure losses of the vapour and liquid. The coefficient of heat transfer in the condensation zone increases with the heating load increasing because the flat mini heat pipe is full of liquid and the exclusion area at the condenser end is small. At a specified heat load, the coefficient of heat transfer at the evaporation zone increases as the temperature of the heat sink increases, while decreasing in the condensation zone. Subsequently, the process of evaporation in the microchannels is improved as the temperature of the heat sink is increased and in the meantime, the process of condensation is modified.

Dual Influences of the Inclination Angle and Heat flux

Experiments were carried out at various angles of inclination of the flat mini heat pipe in order to study the effect of gravitational force. Different positions are selected at a fixed temperature of heat sink $T_{sf} = 35^{\circ}\text{C}$. Figure (10) demonstrates the diversity of thermal resistance versus heat loads, For thermal input power larger than 40 W, the (R_{th}) of the flat mini heat pipe is almost the same for all

the positions taking into account the uncertainties of the thermal resistance, but for heat load lower than 40W, the flat mini heat pipe is sensitive to any change in direction. In

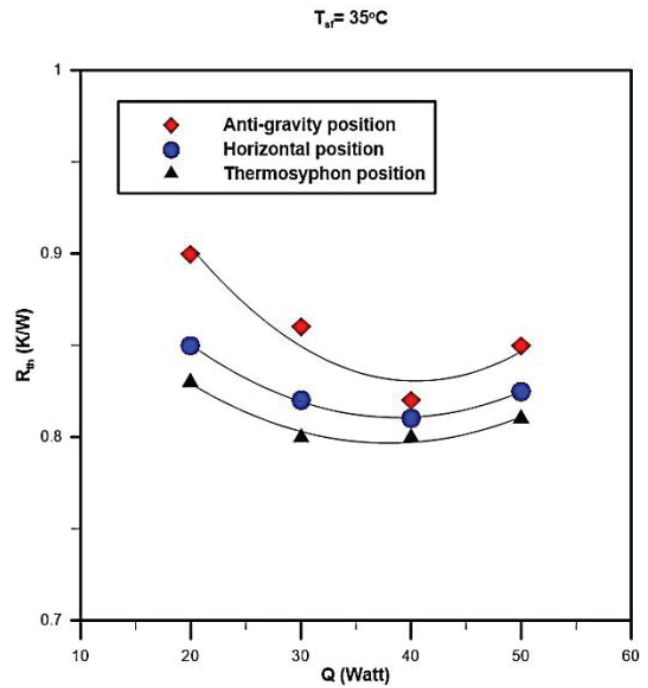


Figure 10. Thermal resistance of flat mini heat pipe versus heat loads in a different direction.

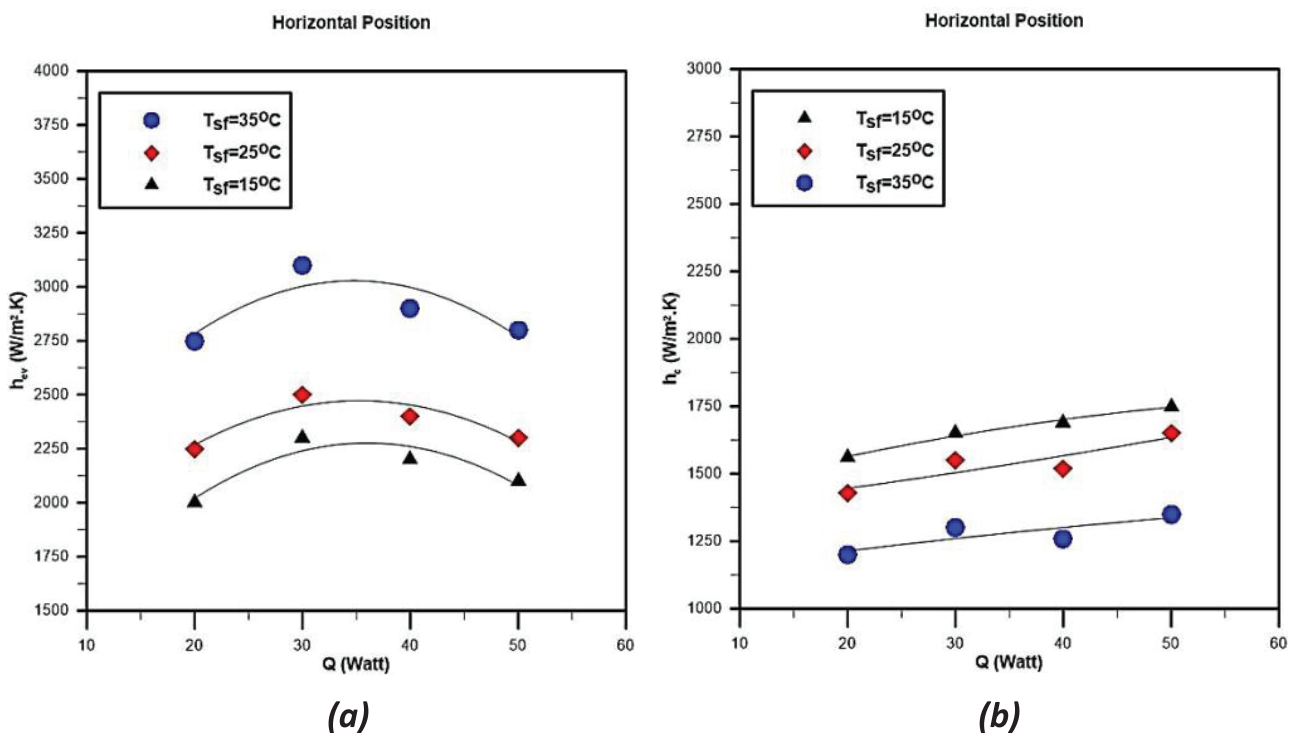


Figure 9. Coefficients of evaporation and condensation heat transfer Vs. heat flux, for various temperatures of heat sink.

fact, the position of thermosyphon displays the lowest thermal resistance, while the position of anti-gravity displays the highest one.

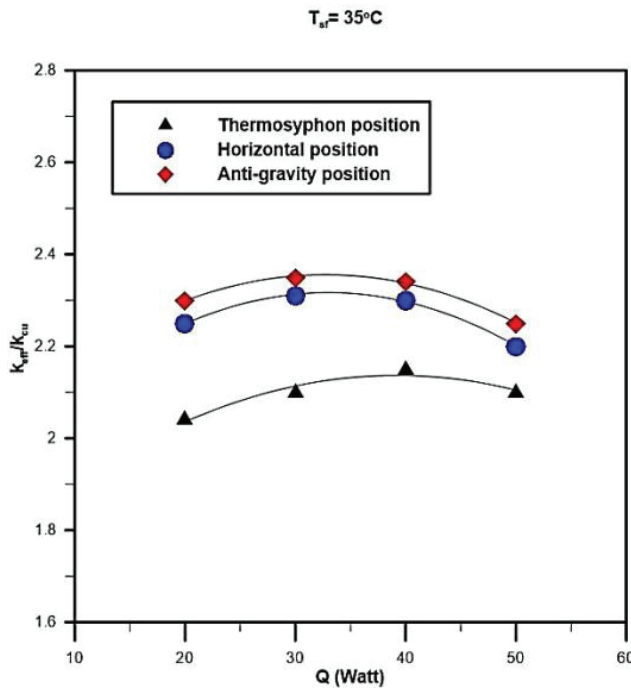


Figure 11. Thermal conductivity ratio improvement as a function of heat loads in a different direction.

Figure (11) shows effective thermal conductivity ratio (k_{eff}/k_{cu}) variations versus heat load. The augmentation rate for the flat mini heat pipe thermal conductivity reached about 240% at a heat load 30W for the positions of thermosyphon and horizontal, while the rate of increase in the case of the anti-gravity situation at a heat load 30W reaches 210%, then the improvement percentage begins to decrease to 200%.

The change in the condenser and evaporator heat transfer coefficient is shown in Figure (12) versus various heat loads. As it is clear in the Figure that the heat transfer coefficient of the evaporator is not much affected by the change in direction of the flat mini heat pipe and when the supplied heat load exceeds the limit of capillary, the coefficient of heat transfer begins to increase for the positions of anti-gravity and horizontal. It can also be seen that the condenser heat transfer coefficient is very sensitive to any change in direction. These results obtained can be interpreted as the position of the thermosyphon is suitable for liquid return to the evaporator.

Uncertainty Error

The uncertainty error of calculating the one dimensional bulk and thermal spreading resistances is estimated from the measured data and the accuracy of the instruments used in the experiments. The accuracy of the J- type thermocouples is 0.5°C, while the average error for power supply reading (wattmeter) is estimated at 2.3W. Therefore, using the single sample analysis [24 and 25], the relative uncertainty error of the thermal resistance is calculated as follows:

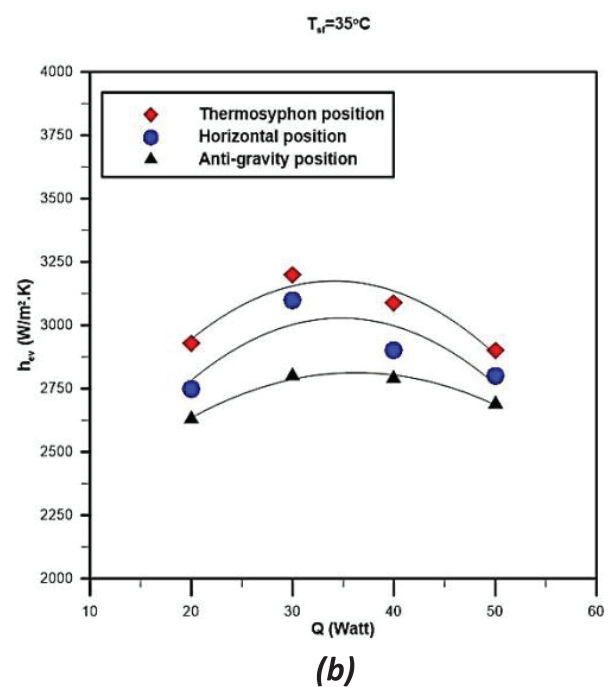
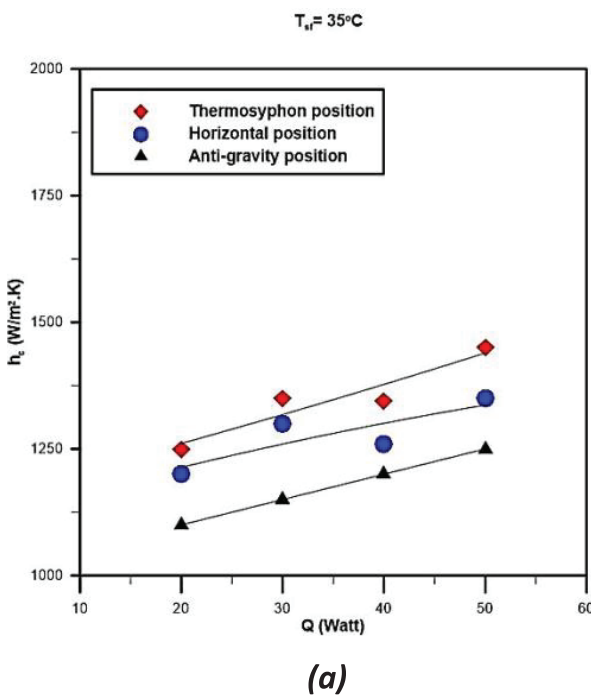


Figure 12. Heat transfer coefficient variations for condensation and evaporation zones as a function of heat loads in different directions.

$$e_R = \sqrt{\left(\frac{e_T}{\Delta T}\right)^2 + \left(\frac{e_Q}{\dot{Q}_H}\right)^2} \quad (9)$$

The relative uncertainty error calculation of the thermal resistances has been limited to the flat miniature heat pipe, as shown in Table 3.

Table 2. Flat miniature heat pipe resistance calculation uncertainty

Heat Load (W)	20	30	40	50
Thermal Resistance Uncertainty (%)	9.6	5	3.1	2.7

CONCLUSION

This work investigated the thermal performance of a flat miniature heat pipe for application in electronics cooling. The temperature measurements allow for a determination of the temperature gradients and maximum localized temperatures for the flat miniature heat pipe. The thermal performance of the FPHPs was further compared to that of copper solid base plates 1mm and 3mm thick. The ability of each sample to dissipate heat was evaluated by measuring the temperature distribution on the mounting surface and the temperature gradient between the heat source and heat sink. From this study the following conclusion is deduced:

1. The obtained laboratory results showed that there is a clear decrease in the temperature gradient and that the highest temperature decreases as compared with a plate of copper for the same dimensions.
2. There was a significant decrease in the temperature difference between the source and the sink with an increase of 240% in the effective thermal conductivity in the case of the horizontal position of the flat mini heat pipe.
3. Important laws of heat have been established in the case of condensation and evaporation, and special mathematical relationships that were used to represent laboratory results and were good at representing the theoretical model in such capillary structures.
4. The experimental data show that the incorporation of the flat mini heat pipe in embedded electronic parts such as computers can enhance the performance of the electronic devices by reducing temperature gradients and increasing thermal conductivity by reducing the number and intensity of hot spots.

NOMENCLATURE

C _p	Specific heat, J/kg. K.
g	Gravity acceleration, m/s ² .
h	Heat transfer coefficient, W/m ² .K.
I	Current, A.
J _a	Modified Jacob's number.

k	Thermal conductivity, W/m. K.
La	Laplace constant, m.
Nu	Nusselt number.
Pr	Prandtl number.
q	Heat flux, W/m ² .
Re	Reynolds number.
t	Thickness, m.
T	Temperature, °C.
T _c	Wall condenser temperature, °C.
T _{ev}	Wall evaporator temperature, °C.
T _{sf}	Heat sink temperature, °C.
V	Voltage, V.
V _e	Velocity, m/s.

Greek Symbols

σ	Surface tension, N/m.
ρ	Density, kg/m ³ .
μ	Dynamic viscosity, kg/m. s.
D _h v	Latent heat of vaporization, J/kg.

Subscripts and superscripts

c	Condenser.
ev	Evaporator.
eff	Effective.
l	Liquid.
sat	Saturation.
sf	Heat sink.
v	Vapour.
w	Wall.

AUTHORSHIP CONTRIBUTIONS

Authors equally contributed to this work.

DATA AVAILABILITY STATEMENT

The authors confirm that the data that supports the findings of this study are available within the article. Raw data that support the finding of this study are available from the corresponding author, upon reasonable request.

CONFLICT OF INTEREST

The author declared no potential conflicts of interest with respect to the research, authorship, and/or publication of this article.

ETHICS

There are no ethical issues with the publication of this manuscript.

REFERENCES

- [1] Xiaowu W, Yong T, Ping C. Investigation into performance of a heat pipe with micro grooves fabricated by extrusion-ploughing process. *Energy Convers Manag* 2009;50:1384–1388. [CrossRef]

- [2] Al-damook A, Azzawi IDJ. The thermohydraulic characteristics and optimization study of radial porous heat sinks using multi-objective computational method. *J Heat Transf* 2021;143:8. [\[CrossRef\]](#)
- [3] Ali SK, Azzawi IDJ, Khadom AA. Experimental validation and numerical investigation for optimization and evaluation of heat transfer enhancement in double coil heat exchanger. *Thermal Sci Eng Prog* 2021;22:100862. [\[CrossRef\]](#)
- [4] Faraj AF, Azzawi IDJ, Yahya SG. Pitch variations study on helically coiled pipe in turbulent flow region using CFD. *Int J Heat Technol.* 2020;38:775–784. [\[CrossRef\]](#)
- [5] Faraj AFF, Azzawi IDJ, Yahya SG, Al-Damook A. Computational fluid dynamics investigation of pitch variations on helically coiled pipe in laminar flow region. *J Heat Transf* 2020;142:10. [\[CrossRef\]](#)
- [6] Do KH, Jang SP. Effect of nanofluids on the thermal performance of a flat micro heat pipe with a rectangular grooved wick. *Int J Heat Mass Transf* 2010;53:2183–2192. [\[CrossRef\]](#)
- [7] Boukhanouf R, Haddad A. Simulation and experimental investigation of thermal performance of a miniature flat plate heat pipe. *Adv Mech Eng* 2013;2013. [\[CrossRef\]](#)
- [8] Tuckerman DB, Pease RFW. High-performance heat sinking for VLSI. *IEEE Electron Device Lett.* 1981. [\[CrossRef\]](#)
- [9] Al-damook A, Alfellag MA, Khalil WH. Three-dimensional computational comparison of mini pinned heat sinks using different nanofluids: Part one-the hydraulic-thermal characteristics. *Heat Transf Asian Res* 2019;49:591–613. [\[CrossRef\]](#)
- [10] Al-damook A, Alfellag MA, Khalil WH. Three-dimensional computational comparison of mini-pinned heat sinks using different nanofluids: Part two-energy and exergy characteristics. *Heat Transf Asian Res* 2020;49:441–460. [\[CrossRef\]](#)
- [11] Khrustlev D, Faghri A. Coupled liquid and vapor flow in miniature passages with micro grooves. *J Heat Transf* 1999;121:729–733. [\[CrossRef\]](#)
- [12] Qu W, Mudawar I. Flow boiling heat transfer in two-phase micro-channel heat sinks--II. Annular two-phase flow model. *Int J Heat Mass Transf.* 2003;46:2773–2784. [\[CrossRef\]](#)
- [13] Steinke ME, Kandlikar SG. An experimental investigation of flow boiling characteristics of water in parallel microchannels. *Trans ASME.* 2004;126. [\[CrossRef\]](#)
- [14] Launay S, Sartre V, Lallemand M. Hydrodynamic and thermal study of a water-filled micro heat pipe array. *J Thermophys Heat Transf* 2004;18:358–363. [\[CrossRef\]](#)
- [15] Saitoh S, Daiguji H, Hihara E. Effect of tube diameter on boiling heat transfer of R134a in horizontal small-diameter tubes. *Int J Heat Mass Transf* 2005;48:4973–4984. [\[CrossRef\]](#)
- [16] Do KH, Kim SJ, Garimella SV. A mathematical model for analyzing the thermal characteristics of a flat micro heat pipe with a grooved wick. *Int J Heat Mass Transf* 2008;51:4637–4650. [\[CrossRef\]](#)
- [17] Bertsch SS, Groll EA, Garimella SV. Effect of heat, mass flux, vapour quality, and saturation temperature on flow boiling heat transfer in microchannels. *Int J Multiphase Flow* 2009;35:142–154. [\[CrossRef\]](#)
- [18] Do KH, Jang SP. Effect of nanofluids on the thermal performance of a flat micro heat pipe with a rectangular grooved wick. *Int J Heat Mass Transf* 2010;53:2183–2192. [\[CrossRef\]](#)
- [19] Fadhil AM, Khalil WH, Al-damook A. The hydraulic-thermal performance of miniature compact heat sinks using SiO₂-water nanofluids. *Heat Transf Asian Res* 2019;48:3101–3114. [\[CrossRef\]](#)
- [20] Fadhil AM, Khalil WH, Al-damook A, Ahmadi MH, Ghalandari M, Yusaf T. Numerical investigation of hydraulic-thermal performance and entropy generation of compact heat sinks with SiO₂-water nanofluids. *Math Methods Appl Sci* 2020. [\[CrossRef\]](#)
- [21] Szczukiewicz S, Borhani N, Thome JR. Two-phase heat transfer and high-speed visualization of refrigerant flows in 100x100 μm² silicon multi-microchannels. *Int J Refrigeration* 2013;36:402–413. [\[CrossRef\]](#)
- [22] Leão HLLS, Do Nascimento FJ, Ribatski G. Flow boiling heat transfer of R407C in a microchannels based heat spreader. *J Exp Thermal Fluid Sci* 2014;59:140–151. [\[CrossRef\]](#)
- [23] Wang HJ, Tsai HC, Chen HK, Shing TK. Capillarity of rectangular micro grooves and their application to heat pipes. *Tamkang J Sci Eng* 2005;8:249–255.
- [24] Kline SJ, McClintock FA. Describing uncertainties in single sample experiments. *Mech Eng* 1953;75:3–8.
- [25] Mohammed K, Saleem A, Obaid ZH. Numerical investigation of Nusselt number for nanofluids flow in an inclined cylinder. *Front Heat Mass Transf* 2021;16. [\[CrossRef\]](#)